ANALYSIS OF A ROTARY ADSORBENT FILTER FOR INDOOR AIR QUALITY CONTROL

Krista M. Knight
Student Member ASHRAE

S.A. Klein, Ph.D.
Member ASHRAE

J.W. Mitchell, Ph.D., P.E.
Member ASHRAE

ABSTRACT

Volatile organic compounds (VOCs) are a common type of indoor air pollutant with individual concentrations typically ranging in the parts per billion (ppb). The usual method for removing VOCs from indoor air is by adsorption on fixed-bed activated carbon filters. These filters have a finite useful lifetime and must be periodically replaced; for some organics, the lifetime is short. By using a rotary configuration, a charcoal filter can be continually regenerated, extending its useful life and possibly allowing removal of a wider range of VOCs. In this paper, the potential of such a configuration is explored through analysis of a rotary regenerative activated carbon wheel with infinite transfer coefficients. As a first approximation, linear isotherms are assumed and interference between multiple adsorbing contaminants is neglected. Design considerations and performance limitations are discussed, including implications for temperature and humidity control.

INTRODUCTION

In response to increasing energy costs and concern over conservation of energy, many buildings, including homes, schools, and office buildings, have been tightened to prevent energy losses through infiltration. At the same time, outdoor ventilation rates have been decreased. While these measures have been successful in reducing energy requirements, problems with the quality of indoor air have resulted in some cases. Studies have shown that the numbers and concentrations of contaminants found in indoor air are much larger than those found in outdoor air (Johansson 1978; Miksch et al. 1982; Berglund et al. 1982a). The number of volatile organic compounds (VOCs) alone is often greater than 100, although the concentrations, which are often in the low ppb range, are several orders of magnitude less than industrial safety limits (Johansson 1978; Miksch et al. 1982; Berglund et al. 1982a,b). Yet complaints about indoor air quality

occur. "Sick building syndrome" is the term used when people complain of minor health problems, such as fatigue, dryness, and headaches. While the irritating effect of each contaminant alone is usually negligible, complex interactions between pollutants, temperature, and humidity can result in irritating sensory stimuli. The method of these interactions is not well understood, such that prediction of indoor air problems from air sample analysis is difficult at best (Miksch et al. 1982; Berglund et al. 1984). Pollutants are emitted from sources within buildings, such as people, building materials, cleaning products, furniture, carpets, copying machines, cigarette smoke, etc.

Traditionally, activated carbon has been used for adsorption of volatile organic compounds. Activated carbon has a relatively nonpolar surface and a wide pore size distribution. Both of these characteristics tend to minimize selective adsorption, thereby making carbon suitable for simultaneously removing many different organics.

The modeling results will be presented as relative concentrations, e.g., the ratio of the outlet concentration to the regeneration inlet concentration, since the exact contaminant concentrations and maximum allowable concentrations are often unknown. Although the modeling results are based on very limited experimental data, the modeling study helps indicate areas for future experimental study.

ISOTHERM DATA

The isotherm data available in the published literature are very limited at the low concentration ranges typically encountered in indoor air quality applications; this lack of data has also been noted by Ramanathan et al. (1988). Furthermore, the low-concentration isotherm data that exist consist mostly of pure component isotherms at room temperature. Much more data are available at higher concentrations, including both pure and multicomponent isotherms and different temperatures, e.g., Lewis et al. (1950), Gonzalez and Holland (1971), and Ray and Box (1950). A recent study

Krista M. Knight is a research assistant in the Solar Energy Laboratory and S.A. Klein and J.W. Mitchell are professors in the Mechanical Engineering Department at University of Wisconsin-Madison.

compiled a list of many sources of isotherm data (Hines et al. 1990).

Six sources of low-concentration isotherm data were found from a literature review, although the data were still at concentrations higher than encountered in indoor air quality problems. Included in the sources of data are nine organic vapors at concentrations ranging upward from roughly 50 ppb (Clapham et al. 1970); acetaldehyde from 2 ppm (Kyle and Eckhoff 1974); methane, ethane, acetylene, acetaldehyde, and acetone at concentrations from 5 ppm (Forsythe 1988); and acetaldehyde, benzene, and 1,1,1-trichloroethane from 100 to 190 ppb (Ramanathan et al. 1988). In another study (Robell et al. 1970), nine different pure component isotherms, including water vapor, at concentrations from 100 ppb were measured; in addition, data were taken for mixtures and multiple temperatures. There are significant differences in the amount adsorbed for some of the data, e.g., the benzene data from Ramanathan et al. (1988) and Clapham et al. (1970) differ by three orders of magnitude.

Trends for adsorption of different contaminants can be obtained from the higher concentration data. In general, for adsorption of organics on activated carbon, the amount adsorbed for a given gas-phase concentration will increase as molecular weight and critical temperature increase (Lewis et al. 1950).

A linear isotherm form will be assumed for the analysis presented here. Theoretically, at very low concentrations, the isotherm should be linear (Hill 1952). Uncertainties involved in the design, e.g., unknown contaminants, low concentrations, and lack of isotherm data, justify the use of a linear isotherm as a first approximation to reality:

$$W = K'p_i = K'Py \approx K'P\omega = K\omega. \qquad (1)$$

The temperature dependence of the isotherm constant, K, can be derived from a phase equilibrium equation analogous to the Clausius-Clapeyron equation, where the heat of adsorption, Δh_s, has been assumed independent of temperature:

$$K = K'P = K_oP\exp\left[\frac{\Delta h_s}{R}\left(\frac{1}{T} - \frac{1}{T_0}\right)\right], \qquad (2)$$

where T_0 and K_0 are a reference temperature and the isotherm slope at the reference temperature, respectively. The reference isotherm slope, K_0, is in units of K', i.e., lbmol/(lbm·atm) (kgmol/(kg·atm)), whereas K is in units of lbmol/lbm (kgmol/kg). At a total pressure of 1 atm, the values of K and K' are identical. In addition, since pressure units of atm are used in this paper for both the I-P and SI units, the K values are identical in the two unit systems.

The range of the isotherm slopes (the isotherm constant) varies considerably for different contaminants. For example, Table 1 lists estimates of the limiting isotherm slopes obtained from the data in Forsythe (1988). The heat of adsorption, Δh, is generally within the range from 3,600 to 18,000 Btu/lbmol (2 to 10 kcal/gmol); somewhat higher values were

Table 1
Extimates of Limiting Isotherm Slopes from Isotherm Data of Forsythe (1988)

Contaminant	K_s lbmol/(lbm·atm) or kgmol/(kg·atm)
Methane	1.8×10^{-3}
Acetylene	2.4×10^{-2}
Ethane	9.0×10^{-2}
Acetaldehyde	2.9
Acetone	1.9×10^{1}
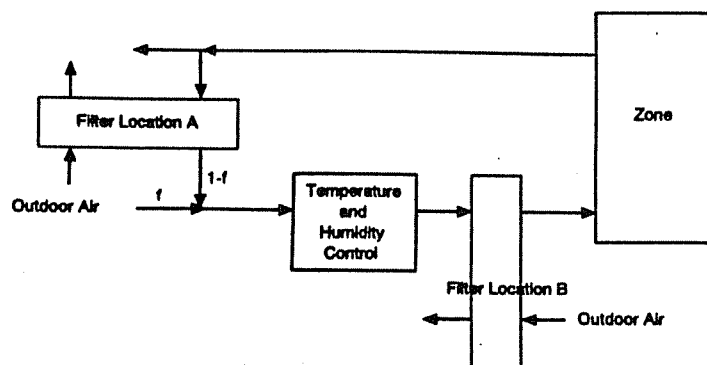
**Figure 2**　　System diagram showing possible filter locations.

reported in Robell et al. (1970), from 18,000 to 30,600 Btu/lbmol (10 to 17 kcal/gmol), from their low-concentration isotherms.

MAXIMUM LIFETIME ESTIMATE

A simple estimate of the maximum lifetime of a fixed-bed adsorption filter can be obtained by assuming that the entire filter is saturated before breakthrough occurs, that there is no interference from other adsorbing contaminants, and that the filter remains at a constant temperature. These assumptions will lead to an overestimate of the actual filter lifetime. Dividing the amount of contaminant adsorbed by the contaminant flow rate gives the estimate of the time until breakthrough:

$$\Theta_B = \frac{m_m W}{\omega \tilde{\rho}_{air} Q}. \qquad (3)$$

As an example, a particular commercially marketed activated carbon filter (CFC) consists of six removable carbon trays inserted in a box-like housing, roughly 1 ft x 2 ft x 2 ft (0.3 m x 0.6 m x 0.6 m). The unit is rated for 1,000 cfm (1,700 m³/h). The weight of carbon in each tray is approximately 10 lb (4.5 kg) (CFC 1992), for a total of 60 lb (27 kg) of carbon in the unit. For the adsorption of benzene at 100 ppb, the reported equilibrium amount adsorbed ranges from 1.24 x
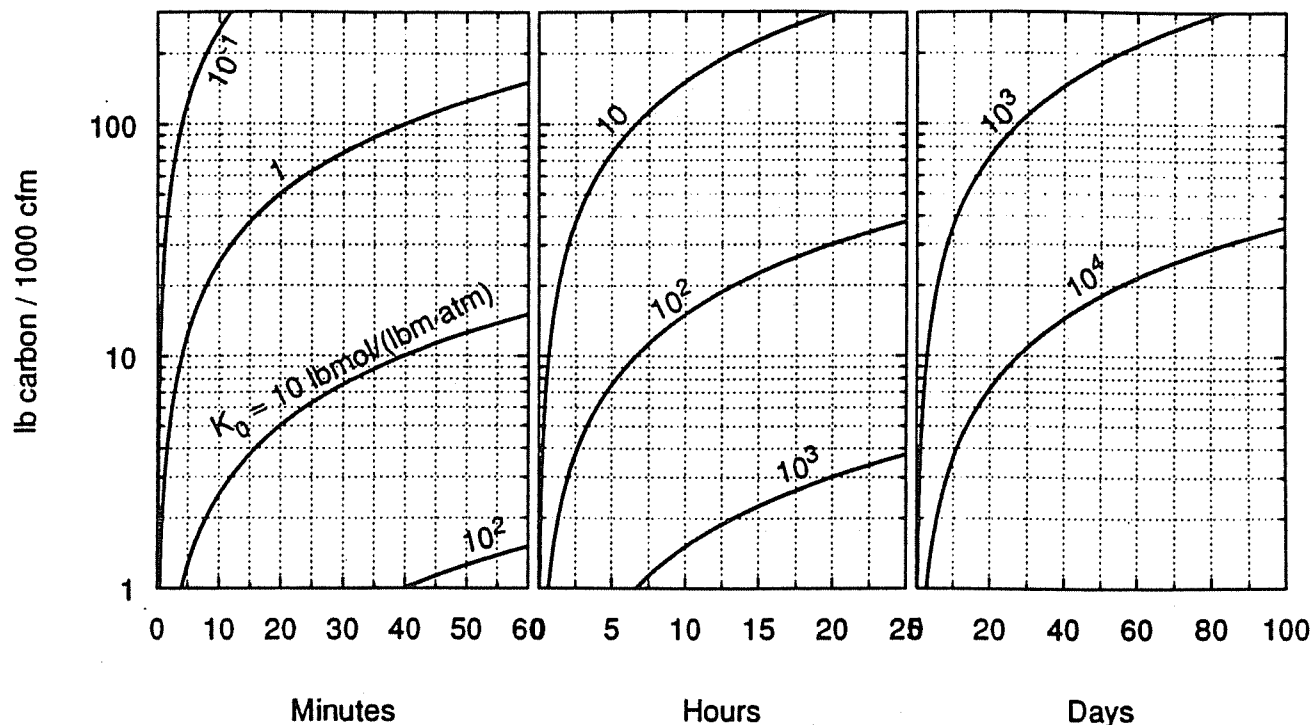
Figure 1 *Maximum fixed-bed filter lifetime estimate for different isotherm slopes at 25°C.*

10^{-7} (Ramanathan et al. 1988) to 2.44 x 10^{-4} (Clapham et al. 1970) lbmol/lbm carbon, depending on the data source. At a temperature of 77°F (25°C) and a flow rate of 1,000 cfm (1,700 m^3/h), the maximum lifetimes, using the two different isotherm values, are 29 minutes and 40 days, respectively. Although 100 ppb may be higher than actual inlet concentrations encountered in indoor air quality situations, within the range where the isotherm is linear the lifetime estimate is independent of inlet concentration. Figure 1 illustrates the maximum lifetime estimate as a function of the pounds of carbon per 1,000 cfm for different isotherm slopes at 77°F (25°C).

The short maximum lifetimes of the fixed-bed carbon filters calls into question their practicality. The frequent replacement or regeneration needed for effective use of a carbon filter indicates that a rotary regenerative configuration, such as used in desiccant air-conditioning systems, may be a more practical solution.

ROTARY REGENERATIVE ACTIVATED CARBON FILTERS

A system diagram for an HVAC system with a rotary regenerative carbon filter is shown in Figure 2. The filter may be located in either the return air (location A) or in the supply air (location B), as in ASHRAE Standard 62-1989 (ASHRAE 1989). Outdoor air is heated and passed through the regeneration portion of the carbon wheel; the heat re-

quired for regeneration could possibly be obtained through solar energy or waste heat reclamation. Although it is not shown as such, it may be necessary to modify the temperature and humidity of the airstream both before and after the carbon filter to improve the filter efficiency.

The adsorbent bed rotates between two different airstreams (see Figure 3); the portions of the bed through which the different airstreams pass are sealed off from each other to prevent mixing. The airstream from which the controlled component (e.g., water vapor, formaldehyde, etc.) is removed is called the process airstream and the portion of the wheel through which it flows is called the process section (or process side or process period). The section of the wheel in which the controlled component is cleaned from the rotating adsorbent is called the regeneration section (or side or period); the cleaning is accomplished by heating the air that passes through the regeneration section, thereby desorbing the matrix. Other wheel sections can also be incorporated, such as a purging section to cool the matrix after regeneration and before processing.

The idea of a rotary regenerative system using activated carbon is not new. Many textbooks have pictures of regenerated carbon wheels (Treybal 1980; Cooper and Alley 1986), although the applications are for solvent recovery and control of VOC emissions from industrial processes; the concentrations are much higher than those encountered in indoor air. The National Aeronautics and Space Administration (NASA) has carried out some experimental studies of regenerative carbon systems for use in spacecraft (McNulty et al.

1977). No modeling studies of a rotary regenerative carbon system were found.

There have, however, been many studies of rotary regenerative wheels (that adsorb water vapor) for use in desiccant air-conditioning systems, both experimental and computational, e.g., (Maclaine-Cross 1974; van den Bulck et al. 1985a,b; van den Bulck 1987; Jurinak 1982; Schultz 1987; Close and Banks 1972). Studies have looked at the effect of contaminants on desiccant performance (Pesaran et al. 1986) and at the ability of desiccant wheels to remove contaminants (Relwani and Moschandreas 1986). There are several differences between the desiccant system and an activated carbon wheel used to remove trace VOCs from indoor air: the concentrations are much lower and there are multiple adsorbing species with a wide range of isotherm slopes. In addition, in designing the system for a building, the identities of the individual VOCs are most likely unknown.

INFINITE TRANSFER COEFFICIENT ANALYSIS

As a first approximation, modeling studies are often performed with infinite heat and mass transfer coefficients, meaning that equilibrium between the gas and solid phases is reached instantaneously; such analyses are often called equilibrium analyses. For example, in an infinite transfer coefficient analysis, an addition of thermal energy to a gas-solid adsorption system would result in instantaneous identical changes in the gas and solid temperatures and instantaneous changes in the gas- and solid-phase contaminant concentrations (to values given by the isotherm for the new temperature). Equilibrium analyses are often used to obtain qualitative estimates of system performance.

The equilibrium analysis of the rotary regenerative carbon wheel follows the equilibrium analysis of desiccant wheels by van den Bulck et al. (1985a), and much of the nomenclature is identical to that used in their work. In developing the equilibrium model, the following assumptions have been made:

* plug flow,
* negligible pressure drop,
* uniform packing,
* no leakage between process and regeneration sides,
* constant specific heats,
* gas-phase storage is negligible,
* no convection in the solid phase,
* fluid and matrix states are uniform in the radial direction,
* adsorption is completely reversible, and
* adiabatic wheel.

In this paper, only the periodic steady-state solution is considered. Depending on the frame of reference, the definition of steady state used to describe the rotary regenerator operation is different. To a stationary observer, as time
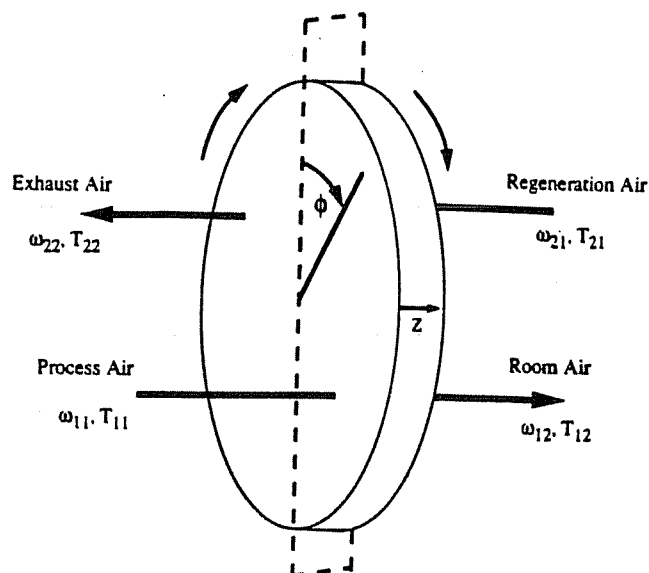

Figure 3   *Rotary regenerative activated carbon wheel.*

passes nothing changes—the concentrations and temperatures at each point on the wheel remain the same. However, to an observer riding on the wheel, the steady-state operation is periodic. The concentrations and temperatures do change with time, although each time the wheel goes around, the same concentrations and temperatures are observed at the same angular position as on the previous rotation.

The different airstreams entering and leaving the rotary filter are denoted by a two-number subscript, the first number indicating which period (1 = process, 2 = regeneration) and the second number indicating which end of the flow (1 = inlet, 2 = outlet). For example, ω_{21} is the regeneration-side inlet gas-phase concentration.

As a result of the assumptions, the filter outlet concentrations and temperatures vary only with angular position. If the wheel rotation speed is slow enough that the outlet state (i.e., concentration and temperature) at the end of the process period is equal to the process inlet state, the wheel is considered to be fully or completely processed. Similarly, if the outlet state at the end of the regeneration period is equal to the regeneration inlet state, the wheel is referred to as fully or completely regenerated.

An additional assumption used in modeling the carbon wheel is that there is no competitive adsorption between the different contaminants. The adsorbed solution theory of Myers and Prausnitz (1965), for low concentrations and linear isotherms predicts that there are no interference effects between the contaminants. This prediction agrees with the theoretical basis for the linear isotherm.

The mass and energy conservation equations for the adsorbent system are as follows.

Contaminant mass conservation equation:

$$\dot{n}_{air}\frac{\partial \omega}{\partial z}+\frac{m_m}{L}\frac{\partial W}{\partial \theta}=0. \qquad (4)$$

FIGURE 4A

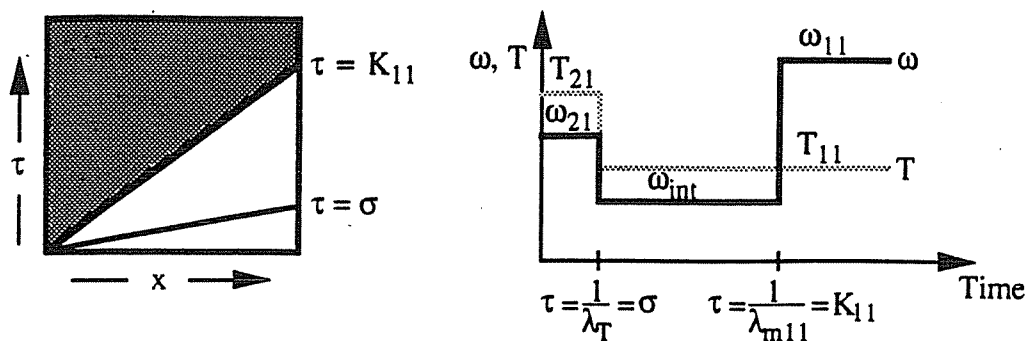Case 1. $\lambda_{m11} < \lambda_{m21} < \lambda_T$, $K_{21} < K_{11} < \sigma$

$\tau = K_{11}$
$\tau = \sigma$

ω, T T_{21} ω_{21} ω_{11} ω T_{11} T ω_{int}

$\tau = \frac{1}{\lambda_T} = \sigma$ $\quad$ $\tau = \frac{1}{\lambda_{m11}} = K_{11}$ $\quad$ Time

FIGURE 4B

Case 2. $\lambda_{m11} < \lambda_T < \lambda_{m21}$, $K_{21} < \sigma < K_{11}$

$\tau = K_{11}$
$\tau = \sigma$
$\tau = K_{21}$

ω, T T_{21} ω_{21} ω_{11} ω T_{11} T ω_{int}

$\tau = \frac{1}{\lambda_{m21}} = K_{21}$ $\quad$ $\tau = \frac{1}{\lambda_{m11}} = K_{11}$ $\quad$ Time

$\tau = \frac{1}{\lambda_T} = \sigma$

FIGURE 4C

Case 3. $\lambda_T < \lambda_{m11} < \lambda_{m21}$, $K_{21} < K_{11} < \sigma$

$\tau = \sigma$
$\tau = K_{21}$

ω, T T_{21} ω_{int} ω_{11} ω ω_{21} T_{11} T

$\tau = \frac{1}{\lambda_{m21}} = K_{21}$ $\quad$ $\tau = \frac{1}{\lambda_T} = \sigma$ $\quad$ Time
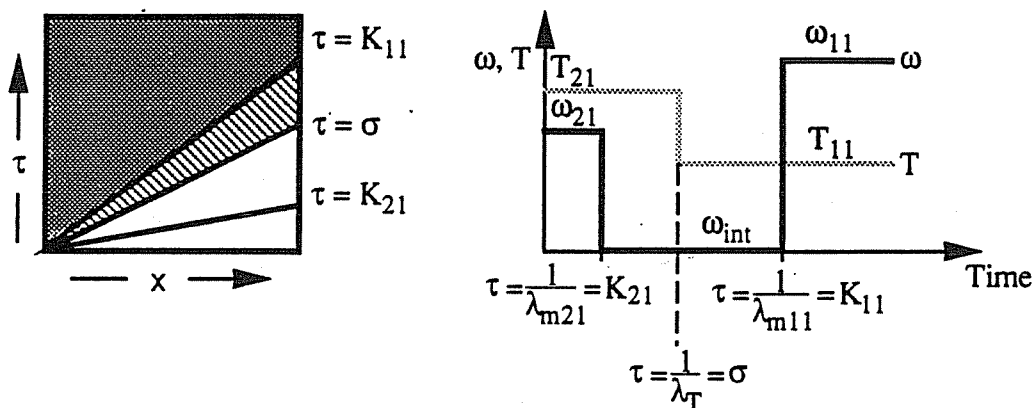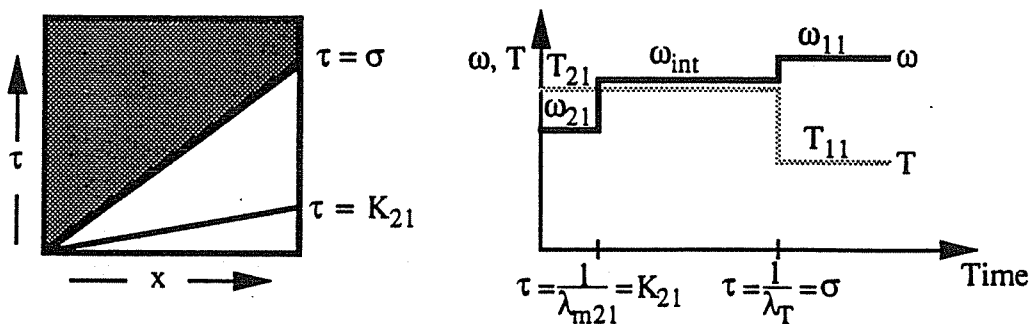
Figure 4 *Equilibrium (infinite transfer coefficients) solution. Wave diagrams and outlet concentration profiles are shown.*

Energy conservation equation:

$$\dot{n}_{air}\frac{\partial h}{\partial z}+\frac{m_m}{L}\frac{\partial H}{\partial \theta}=0. \qquad (5)$$

There are no transfer rate equations due to the assumption of equilibrium. Introducing normalized space and time variables,

$$x = z/L \qquad (6)$$

and

$$\tau = \frac{\Theta \dot{n}_{air}}{m_m}. \qquad (7)$$

Equations 4 and 5 can be rewritten as

$$\frac{\partial W}{\partial \tau}+\frac{\partial \omega}{\partial x}=0 \qquad (8)$$

and

$$\frac{\partial H}{\partial \tau}+\frac{\partial h}{\partial x}=0, \qquad (9)$$

which, along with the following property relations,

$$W = W(\omega, T), \qquad (10)$$

$$h = h(\omega, T), \qquad (11)$$

$$H = H(W, T), \qquad (12)$$

form a system of five equations and five unknowns. The maximum value of the normalized time, τ, occurs at $\Theta = \Theta_j$, where Θ_j is the duration of period j. The parameter $1/\Gamma_j$ is introduced as the upper bound on τ, i.e., $1/\Gamma_j$ is the normalized duration of period j:

$$\frac{1}{\Gamma_j}=\frac{\Theta_j \dot{n}_{air}}{m_m}. \qquad (13)$$

For the rotary regenerative configuration, the initial conditions are as follows:

$$\omega \, (x=0,\tau) \quad = \quad \begin{cases} \omega_{11} & 0<\tau<1/\Gamma_1 \\ \omega_{21} & 1/\Gamma_1<\tau<1/\Gamma_2 \end{cases}, (14)$$

$$T \, (x=0,\tau) \quad = \quad \begin{cases} T_{11} & 0<\tau<1/\Gamma_1 \\ T_{21} & 1/\Gamma_1<\tau<1/\Gamma_2 \end{cases}, (15)$$
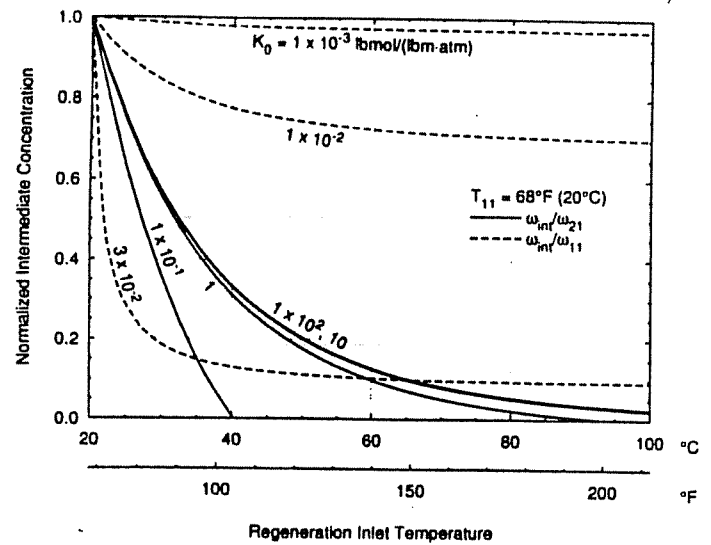
Figure 5   *Normalized intermediate concentration as a function of regeneration inlet temperature.*

where for each period $x = 0$ indicates the inlet side. The step change occurs at the boundaries between the process and regeneration sides.

Equations 8 and 9 form a system of coupled, one-dimensional, nonlinear, hyperbolic partial differential equations, also known as a 2 x 2 system of conservation laws. These equations can be solved using Riemann invariants or other similar techniques (van den Bulck et al. 1985a; Rhee and Amundson 1970, 1972; Rhee et al. 1970; Pan and Basmadjian 1970, 1971; Smoller 1983) and result in changes in temperature and concentration propagating through the matrix as either rarefaction waves or shock waves. The solution is rather complex, requiring an iterative numerical integration procedure.

For the trace contaminant concentrations with which this research is concerned, an assumption in the energy equation greatly simplifies the solution process. The contribution to the total enthalpy from the contaminant, both in the gas phase and in the solid phase, is assumed to be negligible due to the very low concentrations. The gas- and solid-phase enthalpies are approximated as follows:

$$h \approx c_{air}(T - T_{ref}), \qquad (16)$$

$$H \approx c_m(T - T_{ref}). \qquad (17)$$

Physically, this assumption means that the adsorption and desorption processes cause no change in the temperature of the system since the amount of contaminant adsorbed and desorbed is so small.

Using Equations 16 and 17, the energy equation can be expressed in terms of temperature; using the linear isotherm, the mass conservation equation can be expressed in terms of ω:

Table 2
Process Period Solution for a Fully Regenerated Matrix

	Case 1 $\sigma<K_{21}<K_{11}$	Case 2 $K_{21}<\sigma<K_{11}$	Case 3 $K_{21}<K_{11}<\sigma$
Temperatures			
$T = T_{21}$	$(\tau/x)<\sigma$	$(\tau/x)<\sigma$	$(\tau/x)<\sigma$
$T = T_{11}$	$\sigma<(\tau/x)$	$\sigma<(\tau/x)$	$\sigma<(\tau/x)$
Concentrations			
$\omega = \omega_{21}$	$(\tau/x)<\sigma$	$(\tau/x)<K_{21}$	$(\tau/x)<K_{21}$
$\omega = \omega_{int}$	$\sigma<(\tau/x)<K_{11}$	$K_{21}<(\tau/x)<K_{11}$	$K_{21}<(\tau/x)<\sigma$
$\omega = \omega_{11}$	$(\tau/x)>K_{11}$	$(\tau/x)>K_{11}$	$(\tau/x)>\sigma$
Intermediate Concentration			
ω_{int}	$\omega_{21}[(K_{21}-\rho)/(K_{11}-\sigma)]$	0	$\omega_{11}[(K_{11}-\sigma)/(K_{21}-\sigma)]$

$$\frac{\partial\omega}{\partial\tau}+\frac{1}{K}\frac{\partial\omega}{\partial x}=0 \qquad (18)$$

and

$$\frac{\partial T}{\partial\tau}+\frac{1}{\sigma}\frac{\partial T}{\partial x}=0 \ , \qquad (19)$$

where

$$\sigma=\frac{c_m}{c_{air}}. \qquad (20)$$

A very brief explanation of the solution to these equations is presented in this paper; for a more detailed description, see Knight (1992).

For the initial conditions of Equations 14 and 15, the solution to Equations 18 and 19 consists of regions of constant concentration and temperature ("states") separated by waves. Consider the solution for a fully regenerated process period, so that initially the matrix is in equilibrium at state 21; the inlet airstream is at state 11. For now, limit the solution to those values of K_0 and temperatures such that $K > \sigma$. In this case, the solution consists of a "thermal" wave propagating at the speed

$$\lambda_T=\left(\frac{x}{\tau}\right)_T=\frac{1}{\sigma} \qquad (21)$$

and a "mass" wave propagating at the speed

$$\lambda_m=\left(\frac{x}{\tau}\right)_m=\frac{1}{K_{11}} \qquad (22)$$

and, since $K > \sigma$, it is evident that $\lambda_m < \lambda_T$.

The shape of the waves is a discontinuity, similar to a shock wave; the terms "thermal" and "mass" indicate from which conservation equation the wave results. Across the thermal wave, which in this case is the faster wave, there will be a change in temperature from T_{21} to T_{11} and changes in the concentrations from (W_{21}, ω_{21}) to intermediate concentrations (W_{int}, ω_{int}). Across the mass wave, the concentrations change from (W_{int}, ω_{int}) to (W_{11}, ω_{11}), but there is no change in temperature. Figure 4a illustrates a typical solution, with a wave diagram on the left and the temperature and concentration outlet profiles on the right.

The value of the intermediate concentrations can be obtained from a mass balance and, for this case, where the thermal wave is the faster wave,

$$\omega_{int}=\omega_{21}\left[\frac{K_{21}-\sigma}{K_{11}-\sigma}\right] \qquad (23)$$

and

$$W_{int}=K_{11}\omega_{int}=W_{21}\frac{K_{11}}{K_{21}}\left[\frac{K_{21}-\sigma}{K_{11}-\sigma}\right] \qquad (24)$$

At higher concentrations, where the assumption of Equations 16 and 17 is not valid, the temperature would change across the thermal wave from T_{21} to an intermediate temperature, T_{int}, and across the mass wave from T_{int} to T_{11}. Studies have shown that for the low concentrations such as present in indoor air, the assumption appears to be valid (Knight 1992).

The solution given by Equations 21 through 24 is limited to temperatures and isotherm slopes such that $K > \sigma$. Because there are two different temperatures in the problem, T_{21} and T_{11}, there are two different K values, K_{21} and K_{11}. Therefore, there are three different possible situations: case 1: $\sigma < K_{21} < K_{11}$, case 2: $K_{21} < \sigma < K_{11}$, and case 3: $K_{21} < K_{11} < \sigma$.

The thermal wave speed, λ_T, is always equal to $1/\sigma$; in general, there are two possible mass wave speeds, $\lambda_{m11} = 1/K_{11}$ and $\lambda_{m21} = 1/K_{21}$. For the case just described, where $K > \sigma$, the thermal wave speed is greater than either of the mass wave speeds, and since the region behind the thermal wave is at the temperature T_{11}, the only relevant mass wave speed is $\lambda_{m11} = 1/K_{11}$. For case 3, the thermal wave is slower than the mass wave at either temperature and the only relevant mass wave speed is $\lambda_{m21} = 1/K_{21}$. For case 2, the thermal wave is slower than the mass wave at the initial temperature (T_{21}), but faster than the mass wave at the inlet temperature, T_{11}. In this case, there is a mass wave within both constant-temperature regions, and the thermal wave is between the mass waves. Mass and energy balances are used to determine the intermediate concentrations.

A similar analysis can be applied to the regeneration period; however, in this paper only the process period outlet state will be examined. Also, only a fully regenerated carbon wheel will be considered for the analyses, so that upon

entering the process period, the wheel is assumed to be in equilibrium with the regeneration inlet conditions.

PROCESS PERIOD SOLUTION (FULLY REGENERATED MATRIX)

The process period solution for a fully regenerated matrix is presented in Table 2. The top section of Table 2 lists the temperature solution and the middle section lists the concentration solution. The three columns on the right side of Table 2 indicate, for each case, the region in which the temperature or concentration is as specified in the left column. The bottom section of Table 2 lists the value of the intermediate concentration for each case. Figure 4 illustrates wave diagrams and outlet concentration and temperature profiles for the three cases.

The intermediate concentration for case 1 is independent of the process inlet concentration. It depends on the process and regeneration temperatures and the regeneration inlet concentration. Since $K_{21} < K_{11}$, ω_{int} will be less than ω_{21}. If outdoor air is used for the regeneration inlet, this means that some of the air exiting the process side of the filter will actually be cleaner than the outdoor air. For case 2, the intermediate concentration is zero. For case 3, the intermediate concentration depends on the process inlet concentration and temperature and the regeneration inlet temperature; it is independent of the regeneration inlet concentration. In this case, ω_{int} is greater than ω_{11} since $K_{11} > K_{21}$.

The intermediate concentration for $T_{11} = 68°F$ (20°C) for the parameter values listed in Table 3 is plotted as a function of regeneration temperature in Figure 5 for different K_0 values. The ordinate is the normalized intermediate concentration—ω_{int}/ω_{21} for case 1 intermediate concentrations or ω_{int}/ω_{11} for case 3 concentrations. All of the intermediate concentrations decrease with increasing temperature; ω_{int} is zero at regeneration temperatures above 104°F (40°C) for $K_0 = 1 \times 10^{-1}$ lbmol/(lbm·atm). The curves for the two largest isotherm slopes appear to be the same; indeed, in the limit as K_0 goes to infinity, the K values become much larger than ω, and the value of ω_{int}/ω_{21} reaches a limiting value of $\exp[\Delta h/R(1/T_{21} - 1/T_{11})]$, independent of K_0. In the limit as $K_0 \rightarrow 0$, $\omega_{int} \rightarrow \omega_{11}$.

However, the intermediate concentration is the effluent concentration for only a portion of the process outlet. It is ultimately the average outlet concentration over the entire process period that determines the reduction capability of the filter. A low intermediate concentration is desirable, but if it is output for only a small portion of the process period, a somewhat higher intermediate concentration output for a larger portion of the process period may be more advantageous. The process period average outlet concentration is given by

Table 3
Base Parameter Values Used in Calculations

	I-P Units	SI Units
Δh_s	17996 Btu/lbmol	41860 kJ/kgmol
c_m	0.56 Btu/lbm	1.3 kJ/kg
c_{ar}	12.537 Btu/lbmol	29.163 kJ/kgmol
$\sigma = c_m/c_{ar}$	4.458 x 10^{-2}lbmol/lbm	4.458 x 10^{-2} kgmol/kg
T_0	77°F	25°C

$$\omega_{12} = \Gamma_1 \left[\omega_{21} \min\left(\tau_A, \frac{1}{\Gamma_1}\right) + \omega_{int}\left(\min\left(\tau_B, \frac{1}{\Gamma_1}\right) - \tau_A\right)^+ + \omega_{11}\left(\frac{1}{\Gamma_1} - \tau_B\right)^+ \right], \quad (25)$$

$$\tau_A = \min\left(\frac{1}{\Gamma_1}, \sigma, K_{21}\right), \quad (26)$$

and

$$\tau_B = \min\left(\frac{1}{\Gamma_1}, max\left(\sigma, K_{11}\right)\right), \quad (27)$$

where the + superscripts indicate inclusion of the term only if it is positive. τ_A is the breakthrough time of the first wave with which a change in concentration is associated and τ_B is the breakthrough time of the second wave with which a change in concentration is associated. Similarly, the average outlet temperature is given by

$$T_{12} = \Gamma_1 \left[T_{21} \min\left(\sigma, \frac{1}{\Gamma_1}\right) + T_{11}\left(\frac{1}{\Gamma_1} - \sigma\right)^+ \right] \quad (28)$$

Quantities influencing the average outlet states include the duration of the process period $(1/\Gamma_1)$, the various concentrations $(\omega_{11}, \omega_{21}, \omega_{int})$, and the breakthrough times of the various waves (σ, K_{21}, K_{11}). The intermediate concentration, however, can be expressed as a function of the other quantities. Figure 6 shows the average process outlet concentration as a function of process period duration. Each curve represents a different K_0 value (a different contaminant). A longer process period duration is equivalent to a slower rotation speed. For Figure 6, the process inlet concentration has been assumed to be twice the regeneration inlet concentration. The abrupt changes in the slope of the curves indicate a wave
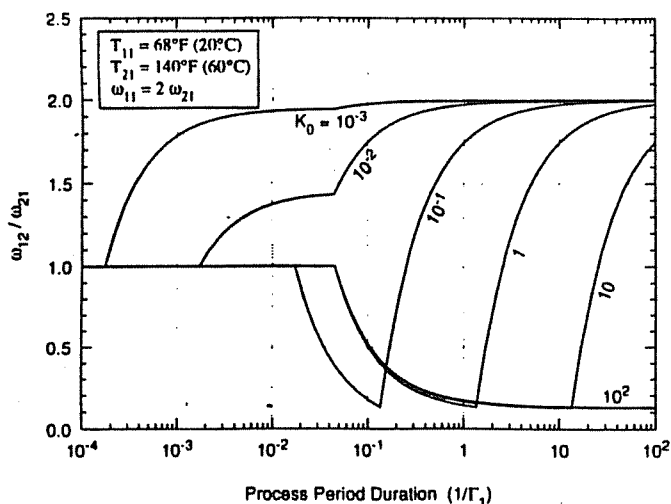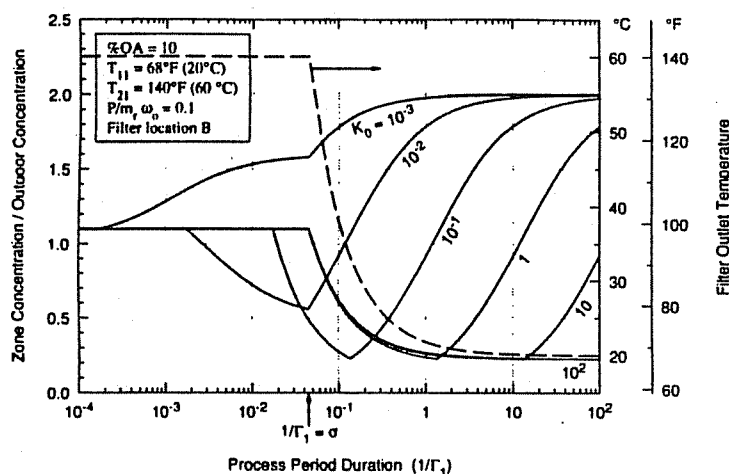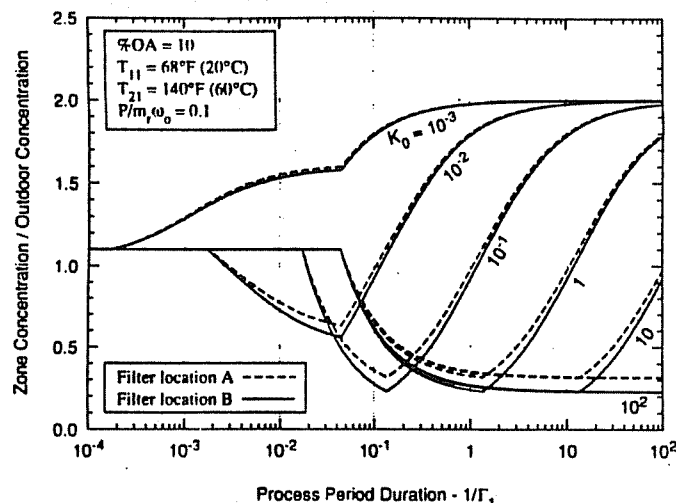
Figure 6   *Process period average outlet concentration as a function of process period duration.*
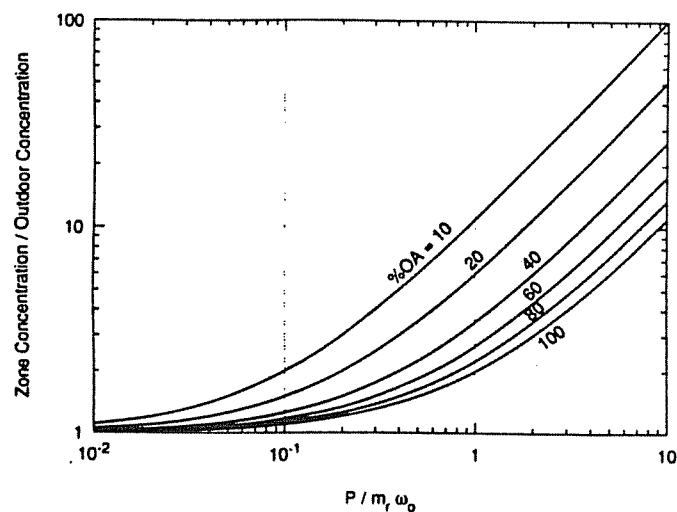
Figure 7   *Zone concentration relative to the outdoor concentration with no filter, as a function of pollutant generation rate.*

Figure 8   *Zone concentration and filter outlet temperature as a function of process period duration for filter at location B.*

Figure 9   *Comparison of zone concentration as a function of process period duration for filters at location A and location B.*

breaking through, so that sudden changes in the instantaneous outlet concentration occur. For example, the curve for $K_0 = 1 \times 10^{-2}$ lbmol/(lbm·atm) represents a case 3 contaminant. The mass wave breaks through at $1/\Gamma_1 = K_{11} = 1.719 \times 10^{-3}$ lbmol/lbm and the temperature wave breaks through at $1/\Gamma_1 = \sigma = 4.458 \times 10^{-2}$ lbmol/lbm.

By rotating the wheel very fast ($1/\Gamma_1$ very small), none of the waves has a chance to break through and the average outlet concentration is equal to the regeneration inlet concentration. Rotating the wheel very slowly means that all of the waves break through very quickly, and the average outlet concentration approaches the process inlet concentration. Any ω_{12}/ω_{11} values below 1 indicate an average outlet concentration below the outdoor concentration.

In the figures shown so far, the process inlet concentration has been assumed to be independent of the process outlet concentration. In reality, changes in the outlet concentration

affect the inlet concentration. By considering the entire system of Figure 2 and assuming outdoor air is used to regenerate the filter, expressions for the steady-state zone concentration (relative to the outdoor concentration) for filters placed in both locations A and B can be developed from mass balances and the equation for the average outlet concentration. A constant pollutant generation rate and perfect mixing of the zone are assumed:

Table 4
Definitions of τ_A, τ_B, α_1, and α_{int} for Use in Equations 29 and 30 (Zone Concentration Equations)

Case	τ_A	τ_B	α_1 — Location A	α_1 — Location B	α_{int}
1: $\sigma < K_{21} < K_{11}$	σ	K_{11}	1	1	$(K_{21} - \sigma)/(K_{11} - \sigma)$
2: $K_{21} < s < K_{11}$	K_{21}	K_{11}	1	1	0
3: $K_{21} < K_{11} < \sigma$	K_{21}	σ	ω_z/ω_o	$f + (1-F)(\omega_z/\omega_o)$	$(K_{11} - \sigma)/(K_{21} - \sigma)$

Filter location A:

$$\frac{\omega_z}{\omega_0} = \frac{\dot{P}}{\dot{m}_r \omega_0} + f + (1 - f)\, \Gamma_1$$

$$\left[\min\left(\tau_A, \frac{1}{\Gamma_1} \right) + \left(\min\left(\tau_B, \frac{1}{\Gamma_1} \right) - \tau_A \right)^+ \alpha_{int}\alpha_1 + \right.$$

$$\left. \left(\frac{1}{\Gamma_1} - \tau_B \right)^+ \frac{\omega_z}{\omega_0} \right]. \qquad (29)$$

Filter location B:

$$\frac{\omega_z}{\omega_0} = \frac{\dot{P}}{\dot{m}_r \omega_0} + \Gamma_1$$

$$\left[\min\left(\tau_A, \frac{1}{\Gamma_1} \right) + \left(\min\left(\tau_B, \frac{1}{\Gamma_1} \right) - \tau_A \right)^+ \alpha_{int}\alpha_1 + \right.$$

$$\left. \left(\frac{1}{\Gamma_1} - \tau_B \right)^+ \left(f + (1 - f)\, \frac{\omega_z}{\omega_0} \right) \right]. \qquad (30)$$

where τ_A, τ_B, α_1, and α_{int} are defined in Table 4. Notice that ω_z/ω_o appears on both sides of the equations.

To estimate the magnitude of the dimensionless generation rate, $\dot{P}/\dot{m}_r\omega_0$, mass balances for a system with no filter are used to relate the generation rate to the zone-to-outdoor-concentration ratio:

$$\frac{\dot{P}}{\dot{m}_r\omega_0} = f\left[\left(\frac{\omega_z}{\omega_0} \right)_{no\ filter} - 1 \right]. \qquad (31)$$

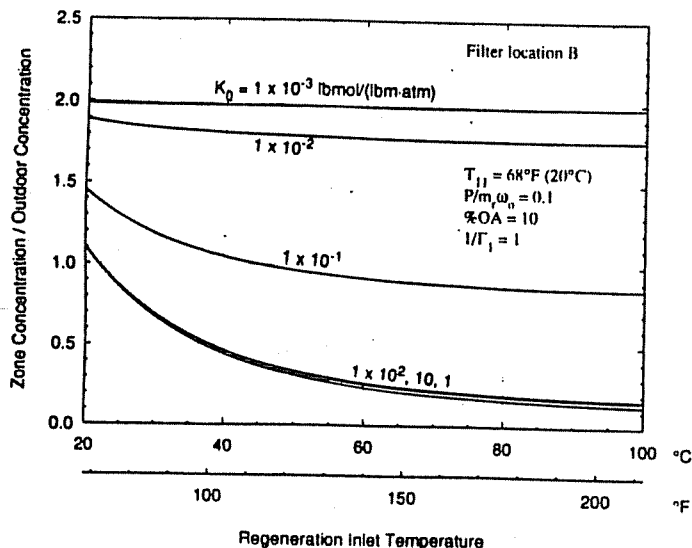Figure 7 illustrates Equation 31 for different amounts of outdoor air.

The zone concentration for a filter at location B, as computed from Equation 30, is shown in Figure 8 as a function of process period duration for $\dot{P}/\dot{m}_r\omega_0 = 0.1$, $T_{11} = 68°F$ (20°C),

$T_{21} = 140°F$ (60°C), and the parameter values listed in Table 3. Each curve represents a different K_0 value. $K_0 = 1, 10,$ and 100 lbmol/(lbm·atm) are case 1, $K_0 = 1 \times 10^{-1}$ lbmol/(lbm·atm) is case 2, and $K_0 = 1 \times 10^{-2}$ and 1×10^{-3} lbmol/(lbm·atm) are case 3. The dashed line represents the filter outlet temperature.

For very fast rotation speeds (small $1/\Gamma_1$), none of the waves has a chance to break through and the filter outlet concentration is equal to the outdoor concentration, so that the zone concentration is equal to that obtained with no filter at 100% outdoor air. For example, from Figure 7, for $\dot{P}/\dot{m}_r\omega_0 = 0.1$, the zone-to-outdoor concentration for no filter at 100% outdoor air is 1.10; in Figure 8, the concentration value for small $1/\Gamma_1$ is 1.10. For slow rotation speeds and small K_0 values, the waves will break through very quickly, so that most of the filter outlet concentration is equal to the filter inlet concentration. The resulting zone concentration is approximately equal to that obtained with no filter at the specified amount of outdoor air. In Figure 8, which is for 10% outdoor air, the concentration values at large $1/\Gamma_1$ for the $K_0 = 10^{-2}$ and $K_0 = 10^{-3}$ lbmol/(lbm·atm) curves are equal to 2.0. As can be seen in Figure 7, 2.0 is the zone-to-outdoor-concentration value for no filter at 10% outdoor air.

The time it takes for the first wave to break through (τ_A from Equation 26) is indicated by the point at which the zone concentration deviates from the no-filter, 100% outdoor air value. For the case 3 contaminants, this is at $1/\Gamma_1 = K_{21}$; for the case 1 and 2 contaminants, this is at σ. Moving along a K_0 curve, the second point at which the slope is discontinuous is the time at which the second wave that affects the concentration breaks through, τ_B. For case 3 contaminants, this is at σ; for cases 1 and 2, it is at K_{11}.

By operating at a rotation speed such that $1/\Gamma_1 > \sigma$, the zone concentration of some of the contaminants (those with larger K_0 values) will be reduced below that possible with no filter at 100% outdoor air. Contaminants with smaller K_0 values will have zone concentrations between the values obtained with no filter at 100% outdoor air and no filter at the specified amount of outdoor air. At rotation speeds such that $1/\Gamma_1 < \sigma$, all of the case 1 contaminants will have zone concentrations equal to that obtained with no filter at 100% outdoor air. The case 2 contaminant concentrations will be
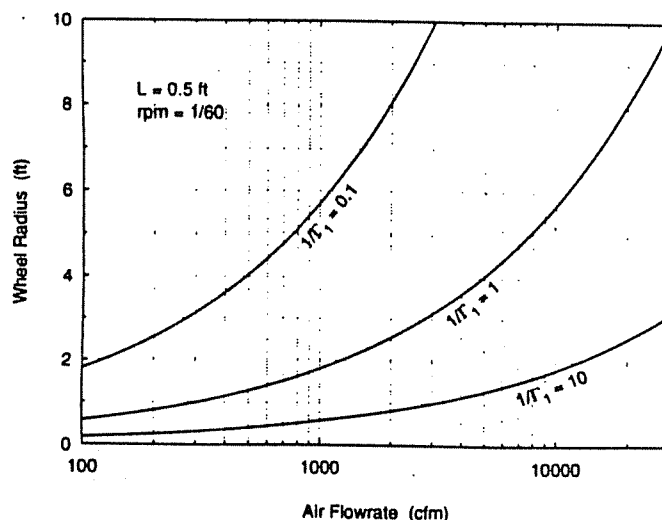
Figure 10   *Zone concentration as a function of regeneration inlet temperature.*

Figure 11   *Example of wheel sizing given the dimensionless process period duration and the air flowrate.*

either less than or equal to the no-filter, 100% outdoor air zone concentration, depending on whether $K_{21} < 1/\Gamma_1$. Case 3 concentrations can be either greater than or less than the no-filter, 100% outdoor zone concentration.

For example, if the wheel were operated such that $1/\Gamma_1 = 1$, for the parameters used in Figure 8, contaminants with $K_0 = 1$, 10, and 100 lbmol/(lbm·atm) (and larger) will have a zone concentration equal to roughly a quarter of the outdoor concentration—this is less than possible with no filter at 100% outdoor air. For a contaminant with $K_0 = 1 \times 10^{-3}$ lbmol/(lbm·atm), the filter would have virtually no effect. For $K_0 = 1 \times 10^{-1}$ lbmol/(lbm·atm), the zone concentration would be slightly less than that obtained with no filter at 100% outdoor air; for $K_0 = 1 \times 10^{-2}$ lbmol/(lbm·atm), the zone concentration would be roughly equal to 1.75 times the outdoor concentration, a value between that obtained with no filter at 100% outdoor air and that obtained with no filter at 10% outdoor air.

Figure 9 compares the effect on the zone concentration when the filter is placed at either location A or B. Location B offers a slight advantage in concentration reduction, although it does require processing a larger amount of air and thus a larger filter. As such, location A may ultimately be preferable. For higher percentages of outdoor air, the effect becomes more pronounced.

The effect of regeneration temperature on the zone-to-outdoor-concentration ratio for a wheel operated at $1/\Gamma_1 = 1$ is shown in Figure 10. Again, $P/m_r\omega_0 = 0.1$, there is 10% outdoor air, and the filter is at location B. From Figure 7, a zone-to-outdoor-concentration ratio of 2.0 is equivalent to the concentration ratio obtained with no filter at 10% outdoor air; a concentration ratio of 1.1 is equivalent to the concentration ratio obtained with no filter at 100% outdoor air. Even at high regeneration temperatures, the filter's ability to remove contaminants with $K_0 = 1 \times 10^{-3}$ lbmol/(lbm·atm) is negligible. The temperature effect is more pronounced for the

larger K_0 values, but it is small for temperatures greater than about 140°F (60°C).

The filter outlet temperature, as seen in Figure 8, is equal to the regeneration temperature for $1/\Gamma_1 < \sigma$. For $1/\Gamma_1 > \sigma$, the outlet temperature decreases from the regeneration temperature to the process temperature. In general, large temperature changes through the filter would require increased processing by the air-conditioning system.

The actual conditions that a filter would see are much more complicated than assumed in this paper. Each contaminant would be generated at a different rate, which would probably not be constant. The heat of adsorption would be different for different contaminants. More graphs illustrating the effect of contaminant generation rate, σ, and Δh_s, along with more detailed studies of the other variables can be found in Knight (1992).

SIZING THE FILTER

Once the operating value of $1/\Gamma_1$ has been selected, a rough estimate of the wheel "size" can be determined. Because this estimate is based on the equilibrium solution, it represents a minimum wheel size. To actually design a filter, an analysis based on finite transfer coefficients would be required and the actual wheel would be larger. This estimate based on the equilibrium solution is used merely to give a feel for the wheel size. Starting with the definition of $1/\Gamma_1$ in Equation 13, the quantities in Equation 13 can be calculated as follows:

$$m_m = \frac{1}{2}\hat{\rho}_c\phi_1 r^2, \qquad (32)$$

$$\Theta_1 = \frac{\phi_1}{\left[\frac{2\pi}{60}\right](rpm)}, \qquad (33)$$

and

$$\dot{n}_{air} = \tilde{\rho}_{air} Q. \qquad (34)$$

Substituting into Equation 13 and solving for the required wheel rotation speed in rpm gives

$$(rpm) = \frac{60\tilde{\rho}_{air}Q}{\pi\hat{\rho}_c\left(\frac{1}{\Gamma_1}\right)}\frac{1}{Lr^2} = \frac{\tilde{\rho}_{air}(cfm)}{\pi\hat{\rho}_c\left(\frac{1}{\Gamma_1}\right)}\frac{1}{L_{ft}r_{ft}^2}(35)$$

The percentage of the wheel designated for processing can be found from the ratio of $1/\Gamma_1$ to $1/\Gamma_2$:

$$\frac{\phi_1}{\phi_2} = \frac{v_{air,2}\left(\frac{1}{\Gamma_1}\right)}{v_{air,1}\left(\frac{1}{\Gamma_2}\right)}. \qquad (36)$$

For a wheel 0.5 ft (0.15 m) thick operating at a rotation speed of one revolution per hour and taking $\hat{\rho}_c = 30$ lbm/ft³ (480 kg/m³) (CCC) and $\tilde{\rho}_{air} = 0.00256$ lbmol/ft³ (0.0409 kgmol/m³), Figure 11 illustrates the required wheel radius for several values of $1/\Gamma_1$.

EXAMPLE CALCULATION

Suppose that one wished to add a rotary regenerative carbon filter at location B of an existing system to lower the indoor concentration of a contaminant with $K_0 = 1$ lbmol/(lbm·atm). The current indoor concentration of the contaminant is twice that of outdoors, the system operates at 10% outdoor air, and the total airflow rate is 3,000 cfm (5,100 m³/h). From Figure 7, the dimensionless pollutant generation rate is 0.1; if the amount of outdoor air were increased to 100%, the zone concentration would be reduced to 1.1 times the outdoor concentration.

Assuming the parameter values listed in Table 3 and an air temperature of 68°F (20°C) entering the filter, the $K_0 = 1$ lbmol/(lbm·atm) curve in Figure 8 shows the zone-to-outdoor concentration as a function of process period duration for a regeneration temperature of 140°F (60°C). Operating at $1/\Gamma_1 = 1$ will give near-optimal performance for the specified contaminant. The zone concentration would be reduced to 0.238 times the outdoor concentration, which is between one-fifth and one-fourth of the zone concentration that could be achieved with no filter at 100% outdoor air. The $K_0 = 1$ lbmol/(lbm·atm) curve in Figure 10 illustrates the effect of

regeneration temperature. If the regeneration temperature were 104°F (40°C) instead of 140°F (60°C), the zone concentration would increase to 0.324 times the outdoor concentration. For a 0.5 ft (0.15 m) thick wheel with a rotation speed of one revolution per hour, the required wheel radius (from Figure 11) is 3.13 ft (0.954 m). If the filter had been placed at location A instead of B, the airflow rate through the filter would be only 2,700 cfm (4,590 m³/h), and the required wheel radius would be reduced to 2.96 ft (0.902 m).

These calculations were based on the assumption of infinite heat and mass transfer coefficients, and as such only represent a "best possible" estimation of the filter performance. For a real system, where the transfer coefficients are finite, higher regeneration temperatures and a larger filter wheel would be required.

CONCLUSIONS

Graphs such as Figure 8 help establish the potential of the rotary regenerative carbon filter. However, these figures (and the calculations on which they are based) are for infinite transfer coefficients. In actual operation, with finite transfer coefficients, larger wheels and higher regeneration temperatures would be required. There are many practical difficulties that need to be overcome, e.g., there is always the possibility that some contaminant might foul the carbon, leaving the filter useless. Studies need to be conducted to determine if adsorption of VOCs on activated carbon is completely reversible. It is unknown whether there are competitive adsorption effects at the very low concentrations of VOCs in indoor air. Experimental work to determine low-concentration isotherms of various organic compounds is necessary, including consideration of multiple contaminants and temperatures other than room temperature.

Operating at a slow enough rotation speed will limit the air temperature change as it passes through the carbon wheel and keep the effect on the heating and cooling requirements small. However, for some of the organics with smaller isotherm slopes, operation in this region will prevent any significant concentration reduction. It is relatively well known that water vapor at relative humidities greater than about 50% will have a detrimental effect on the ability of activated carbon to adsorb organics (Turk 1968); it may be necessary to control the humidity to keep it below this level as it enters the wheel.

Based on the analysis presented, the concept of a rotary regenerative carbon filter has potential as a practical method for removing some of the VOCs (those with large K_0 values) present in indoor air. It is difficult to specify exactly which organics, as the K_0 values for many organics are unknown. In general, organics with larger molecular weights and higher critical temperatures are more likely to be effectively removed by the filter.

NOMENCLATURE

c_{air} = specific heat of the air, Btu/(lbmol air•°F) or J/(kgmol air•K).

c_m = specific heat of the matrix, Btu/(lbm matrix•°F) or J/(kg matrix•K)

(cfm) = volumetric flow rate of the air, cfm

f = fraction of outdoor air

h = enthalpy of the gas phase, Btu/(lbmol clean air) or J/(kgmol clean air)

H = enthalpy of the solid phase, Btu/(lbm clean matrix) or J/(kg clean matrix)

Δh_s = differential isosteric heat of adsorption, Btu/(lbmol i) or J/(kgmol i)

K_0 = isotherm slope at the reference temperature, (lbmol air)/(lbm mtx•atm) or (kgmol air)/(kg mtx•atm)

K = isotherm slope, (lbmol air)/(lbm mtx) or (kgmol air)/(kg mtx)

L = length of the matrix in the flow direction, ft or m

L_{ft} = length of the matrix in the flow direction, ft

m_m = mass of clean adsorbent, lbm clean adsorbent or kg clean adsorbent

$\dot{m}$ = mass flow rate of the air supplied to the zone, lbm/s or kg/s

$\dot{N}_{air}$ = molar flow rate of clean air, lbmol/s or kgmol/s

p_i = partial pressure of contaminant i, (mol i•atm)/(mol i+air)

P = total pressure, atm

$\dot{P}$ = pollutant generation rate, lbmol/s or kgmol/s

Q = total volumetric flow rate of air, (ft³ air)/s or (m³ air)/s

r = wheel radius, ft or m

r_{ft} = wheel radius, ft

R = ideal gas constant, Btu/(lbmol•°F) or J/(kgmol•K)

(rpm) = wheel rotation speed, rpm

T = temperature, °F or °C

T_0 = reference temperature for isotherm slope; in this paper, T_0 = 77°F or 25°C

T_{ref} = reference temperature for enthalpy calculations, °F or °C

v_{air} = air velocity, ft/s or m/s

W = amount of contaminant adsorbed per unit mass of adsorbent, (lbmol i)/(lbm mtx) or (kgmol i)/(kg mtx)

x = dimensionless axial distance

y_i = contaminant mole fraction, (mol i)/(mol i+air)

z = axial distance, ft or m

$1/\Gamma$ = normalized period duration, (lbmol air)/(lbm matrix) or (kgmol air)/(kg matrix)

ϕ_j = angle of the wheel taken up by period j, radians

$\tilde{\rho}_{air}$ = density of the air, lbmol/ft³ or kgmol/m³

$\hat{\rho}_c$ = bulk density of the granular activated carbon, lbm/ft³ or kg/m³

σ = c_m/c_{air}, the specific heat ratio; (lbmol air)/(lbm matrix) or (kgmol air)/(kg matrix)

Θ = time, s

Θ_1 = duration of the process period, s

Θ_B = breakthrough time, s

τ = normalized time, (lbmol air)/(lbm matrix) or (kgmol air)/(kg matrix)

ω = gas-phase contaminant concentration, (lbmol i)/(lbmol clean air) or (kgmol)/(kgmol)

Subscripts

11 = process-side inlet
12 = process-side outlet
21 = regeneration-side inlet
22 = regeneration-side outlet
int = intermediate state
o = outdoor
z = zone

REFERENCES

ASHRAE. 1989. ASHRAE Standard 62-1989, Ventilation for acceptable indoor air quality. Atlanta: American Society of Heating, Refrigerating and Air-Conditioning Engineers, Inc.

Berglund, B., I. Johansson, and T. Lindvall. 1982a. The influence of ventilation on indoor/outdoor air contaminants in an office building. *Environment International* 8: 395-399.

Berglund, B., U. Bergland, T. Lindvall, and H. Nicander-Bredburg. 1982b. Olfactory and chemical characterization of indoor air. Towards a psychophysical model for air quality. *Environment International* 8: 327-332.

Berglund, B., U. Berglund, and T. Lindvall. 1984. Characterization of indoor air quality and sick buildings. *ASHRAE Transactions* 90: 1045-1055.

CCC. Type BPL granular carbon: Mesh sizes: 4 x 6 and 4 x 8. Bulletin 27-118a. Pittsburgh, PA: Calgon Carbon Corporation.

CFC. Purecel and side-carb activated carbon air purifiers specifications guide, Bulletin 19-196. Syracuse, NY: Cambridge Filter Corporation.

CFC. 1992. Personal communication. Syracuse, NY: Cambridge Filter Corporation.

Clapham, T.M., T.J. Junker, and G.S. Tobias. 1970. Activated carbon-odorant removal from air quantified. *ASHRAE Transactions* 76: 75-86.

Close, D.J., and P.J. Banks. 1972. Coupled equilibrium heat and single adsorbate transfer in fluid flow through a porous medium—II. Predictions for a silica-gel air-drier using characteristic charts. *Chem. Eng. Sci.* 27: 1157-1169.

Cooper, C.D., and F.C. Alley. 1986. Air pollution control: A design approach. Boston: PWS Publishers.

Forsythe, R.K., Jr. 1988. Adsorption and dispersion of selected organic gases flowing through activated carbon adsorber beds. Ph.D. thesis, Kent State University, Kent, OH.

Gonzalez, A.J., and C.D. Holland. 1971. Adsorption of equilibria of the light hydrocarbon gases on the activated carbon and silica gel. *AIChE Journal* 17(2): 470-475.

Hill, T.L. 1952. Theory of physical adsorption. *Advances in Catalysis* 4: 211-258.

Hines, A.L., T.K. Ghosh, S.K. Loyalka, and R.C. Warder, Jr. 1990. Investigation of co-sorption of gases and vapors as a means to enhance indoor air quality. Phase I Report. Literature Review. University of Missouri-Rolla, GRI-90/0194.

Johansson, I. 1978. Determination of organic compounds in indoor air with potential reference to air quality. *Atmospheric Environment* 12: 1371-1377.

Jurinak, J.J. 1982. Open cycle desiccant cooling—component models and system simulations. Ph.D. thesis, University of Wisconsin-Madison.

Knight, K.M. 1992. Analysis and design of adsorptive processes for air quality control. Ph.D. thesis, University of Wisconsin-Madison.

Kyle, B.G., and N.D. Eckhoff. 1974. Odor removal from air by adsorption quantified. Kansas State University, technical report prepared for the National Environmental Research Center, EPA-650/2-74-084, PB-236-928.

Lewis, W.K., E.R. Gilliland, B. Chertrow and W.P. Cadogan. 1950. Adsorption equilibria: Pure gas isotherms. *Ind. Eng. Chem.* 42(7): 1326-1332.

Maclaine-Cross, I.L. 1974. A theory of combined heat and mass transfer in regenerators. Ph.D. thesis, Monash University, Australia.

McNulty, K.J., R.L. Goldsmith, G.A. Goldsmith, P.R. Hoover, J. Nwankwo, and A. Turk. 1977. Evaluation of techniques for removal of spacecraft contaminants from activated carbon. NASA CR-151968, N77-20159. Wilmington, MA: Walden Division, of Abcor, Inc.

Miksch, R.R., C.D. Hollowell, and H.E. Schmidt. 1982. Trace organic chemical contaminants in office spaces. *Environment International* 8: 129-137.

Myers, A.L., and J.M. Prausnitz. 1965. Thermodynamics of mixed-gas adsorption. *AIChE J.* 11(1): 121-127.

Pan, C.Y., and D. Basmadjian. 1970. An analysis of adiabatic sorption of single solutes in fixed beds: Pure thermal wave formation and its practical implications. *Chem. Eng. Sci.* 25: 1653-1664.

Pan, C.Y., and D. Basmadjian. 1971. An analysis of adiabatic sorption of single solutes in fixed beds: equilibrium theory. *Chem. Eng. Sci.* 26: 45-47.

Pesaran, A.A., T.M. Thomas, T.R. Penney, and A.W. Czanderna. 1986. Methods to quantify contamination effects on silica gel samples. SERI/TR-252-2802. Golden, CO: Solar Energy Research Institute.

Ramanathan, K., V.L. Debler, M. Kosusko, and L.E. Sparks. 1988. Evaluation of control strategies for volatile organic compounds in indoor air. *Environmental Progress* 7(4): 230-235.

Ray, G.C., and E.O. Box. 1950. Adsorption of gases on activated charcoal. *Ind. Eng. Chem.* 42(7): 1315-1318.

Relwani, S.M., and D.J. Moschandreas. 1986. Indoor pollutant control capabilities of a desiccant dehumidifier system. GRI 86/0200. Chicago, IL: Gas Research Institute.

Rhee, H.-K., and N.R. Amundson. 1970. An analysis of an adiabtic adsorption column: Part I. Theoretical development. *Chem. Engng. J.* 1: 241-254.

Rhee, H.-K., and N.R. Amundson. 1972. An analysis of an adiabtic adsorption column: Part IV. Adsorption in the high temperature range. *Chem. Engng. J.* 3: 121-135.

Rhee, H.-K., E.D. Heerdt, and N.R. Amundson. 1970. An analysis of an adiabatic adsorption column: Part II. Adiabatic adsorption of a single solute. *Chem. Engng. J.* 1: 279-290.

Robell, A.J., C.R. Arnold, A. Wheeler, G.J. Kersels, and R.P. Merrill. 1970. Trace contaminant adsorption and sorbent regeneration. NASA CR-1582, N70-38501. Palo Alto, CA: Lockheed Missiles and Space Company.

Schultz, K.J. 1987. Rotary solid desiccant dehumidifiers. Analysis of models and experimental investigation. Ph.D. thesis, University of Wisconsin-Madison.

Smoller, J. 1983. Shock waves and reaction-diffusion equations. New York: Springer-Verlag.

Treybal, R.E. 1980. Mass-transfer operations. New York: McGraw-Hill.

Turk, A. 1968. Source control by gas-solid adsorption and related processes. In *Air Pollution Vol.III*: Sources of Air Pollution and Their Control, 2d ed., A.C. Stern, ed. pp. 497-519. New York: Academic Press.

van den Bulck, E., J.W. Mitchell, and S.A. Klein. 1985a. Design theory for rotary heat and mass exchangers—I. Wave analysis of rotary heat and mass exchangers with infinite transfer coefficients. *Int. J. Heat Mass Transfer* 28(8): 1575-1586.

van den Bulck, E., J.W. Mitchell, and S.A. Klein. 1985b. Design theory for rotary heat and mass exchangers—II. Effectiveness-NTU method for rotary heat and mass exchangers. *Int. J. Heat Mass Transfer* 28(8): 1587-1595.

van den Bulck, E. 1987. Convective heat and mass transfer in compact regenerative heat exchangers. Ph.D. thesis, University of Wisconsin-Madison.